# NEW SINGLE-LAYERED LINEAR-TO-CIRCULAR POLARIZERS FOR S-BAND CUBESAT APPLICATION

by

**HIDAYATH MIRZA**
**(1640812194)**

A thesisthesis submitted in fulfillmentfulfillment of the requirements for the degree of
Doctor of Philosophy Doctor of Philosophy

**School of Computer & Communication Engineering**
**UNIVERSITI MALAYSIA PERLIS**

2019

## ACKNOWLEDGMENT

My Lord Almighty Allah: I want to express my eternal profound gratitude for blessing me with uncountable bounties each and every moment of my life.

To my forever encouraging and always the enthusiastic, my lovely mother & father, Mrs. Mushraf Sultana and Mr. Sajjad Mirza: I would like to express my love and respect. Without their support, I could not have anything in my life.

To my beloved wife: I would like to express my gratitude for her persistent moral and emotional support. I would also like to thank, my brother Mr. Mehmood Mirza and sister Mrs. Shaista Sultana for his emotional support during my whole study. Also, I would like to thank my brothers-in-law, Mr. & Mrs. Najam for taking care of my family during my stay at UniMap and Mr. Mohammed Nasir for motivating and enthusiasm to join Ph.D.

Moreover, I would like to thank my supervisor Associate Professor Dr. Ping Jack Soh for helping throughout this research work. He has always steered me in the right direction. This degree would be merely impossible to bring into the light, without his support.

Finally, I want to thank all the members of ACE (Advanced Communication Engineering Centre) assistance to this work especially, Mr. Toufiq Md Hossain and Dr. Rizwan Khan Jadoon and Mr. Rais Ahmad Sheikh.

.

## TABLE OF CONTENTS

## LIST OF TABLES

## LIST OF FIGURES

## LIST OF ABBREVIATIONS

| | |
|---|---|
| ADS | Advanced Design System |
| ANGKASA | National Space Agency of Malaysia |
| AR | Axial Ratio |
| CP | Circularly Polarization |
| CST | Computer Simulation Technology |
| EBG | Electromagnetic Band Gap |
| FCC | Federal Communications Commission |
| FSS | Frequency Selective Surfaces |
| GPS | Global Positioning System |
| LHCP | Left Handed Circular Polarization |
| LP | Linearly Polarization |
| LPW | Linearly Polarized Wave |
| MS | Metasurface |
| PDMS | Polydimethylsiloxane |
| RHCP | Right Handed Circular Polarization |
| 3dBFBW | 3dB Axial Ratio BandWidth |

## LIST OF SYMBOLS

| | |
|---|---|
| $(BW)_{CE}$ | Fractional bandwidth with at least 90% conversion efficiency |
| $(BW)_{3dB}$ | Fractional bandwidth with at least 3 dB axial ratio |
| $\theta$ | Angle of incidence of linearly polarized wave |
| $\eta$ | Ellipticity of the output of polarizer |
| $\eta_{conv}$ | Conversion efficiency of the polarizer |
| $C_+$ | Left hand circular polarization |
| $C_-$ | Right hand circular polarization |

**Pengutub Linear-ke-Bulat Lapisan Tunggal Baharu bagi Aplikasi CubeSat Jalur-S**

## ABSTRAK

Pengutub linear ke bulat (LCP) merupakan suatu alternatif yang lebih mudah untuk mencapai pengutuban bulat (CP) berbanding merekabentuk antena CP yang lebih rumit. LCP membolehkan antena berkutub linear (LP) digunakan dengan gandaan tinggi dan lebarjalur luas untuk aplikasi seperti CubeSat. Salah satu cabaran aplikasi ini adalah dalam memastikan CubeSat dapat menampung saiznya bagi kegunaan jalur-S. Salah satu alternatif adalah dengan memastikan LCP tersebut boleh disimpan dalam bentuk yang padat semasa pelancaran CubeSat, sebelum diserakkan untuk kegunaan di angkasa. Namun demikian, kebanyakan LCP sedia ada direka di atas substrat tegar. Bagi memperkenalkan struktur yang fleksibel sepenuhnya dan berprofil rendah, dua jenis bahan telah digunakan dalam projek ini bagi mereka LCP yang berlainan. LCP pertama direka di atas tekstil, yang merupakan suatu kombinasi felt sebagai substrat dan ShieldIt Super sebagai elemen konduktif. Sepertimana yang pertama, kombinasi kedua turut menggunakan ShieldIt Super, dan diimplementasi di atas substrat polydimethylsiloxane (PDMS). LCP-LCP tersebut telah direka berdasarkan dua kategori sel unit, iaitu (a) jenis pejal (dua jenis) dan (b) jenis gelung (dua jenis). Pengutub-pengutub ini telah dinilai menerusi simulasi dan pengukuran dari segi: i) kecekapan penukaran, yang didefinisikan sebagai batas 90 % ke atas kecekapan penukaran, dan lebarjalur pecahannya $(BW)_{CE}$ ; serta ii) nisbah paksi (AR) dengan had 3 dB dan lebarjalur pecahannya $(BW)_{3\,dB}$. Empat LCP yang telah direka dikategorikan berdasarkan bilangan lapisan tekstil konduktifnya, iaitu: (i) rekabentuk dwi-lapisan (tiga jenis) dan (ii) rekabentuk lapisan tunggal (satu jenis). Sel unit jenis pejal direka berdasarkan i) struktur swastika dengan saiz 51.7 × 59.8 × 3.34 mm$^3$ ($0.49\lambda_g \times 0.57\lambda_g \times 0.03\lambda_g$ ); dan ii) struktur sel ternyahbeban dengan saiz 46 × 56.17 × 3.34 mm$^3$ ($0.60\lambda_g \times 0.73\lambda_g \times 0.04\lambda_g$). Manakala sel unit jenis gelung direka berdasarkan: iii) dedekagon bersilang dengan saiz 54 × 64 × 3.34 mm$^3$ ($0.51\lambda_g \times 0.61\lambda_g \times 0.03\lambda_g$ ); dan iv) gelung segiempat sama dan bersaiz 48 × 46 × 3.34 mm$^3$ ($0.45\lambda_g \times 0.43\lambda_g \times 0.03\lambda_g$ ). Rekabentuk sel unit dodekagon bersilang menunjukkan lebarjalur pecahan $(BW)_{CE}$ tertinggi, iaitu 48.12 % (daripada 1.578 GHz hingga 2.578 GHz), berbanding 23.88 % (daripada 2.36 GHz hingga 3 GHz) dan 47.34% (daripada 1.58 GHz hingga 2.56 GHz) yang masing-masing dihasilkan oleh sel unit ternyahbeban dan gelung segiempat sama. Manakala $(BW)_{3\,dB}$ tertinggi yang diukur adalah 33.57% (from 1.71 GHz to 2.4 GHz) yang diukur pada sel unit gelung segiempat sama, diikuti oleh sel unit ternyahbeban 32.64 %, rekabentuk dodekagon bersilang dengan 29.09% and sel swastika dengan lebarjalur sebanyak 1.64 %. Bagi menilai prestasi setelah diintegrasikan dengan mekanisma serakan, prestasi pengutub tersebut turut dinilai semasa dilentur serta semasa disinari pada sudut-sudut serong yang berbeza. Secara amnya, sel unit jenis gelung menunjukkan prestasi yang lebih baik berbanding sel unit jenis pejal

**New Single-Layered Linear-to-Circular Polarizers for S-Band CubeSat Application**

## ABSTRACT

Linear-to-Circular Polarizer (LCP) is considered as a simpler alternative to achieve circular polarization (CP) characteristics compared to designing CP antenna with complex topologies. LCP allows the use of linearly polarized (LP) antennas in CP with considerably higher gain and wider bandwidth for applications such as CubeSats. One of the most challenges of this application is the need for it to be sufficiently compact for operation in the S-band. An alternative is to ensure that the LCP can be stowed in a compact form during the CubeSat's launch and be deployed for use in space. However, current polarizers are mostly designed using rigid substrates. To introduce a fully flexible and low-profile structure, two different conformal materials are used in this project to design different types of LCPs. The first is on textiles, which is a combination of felt as the substrate and ShieldIt Super as the conductive element. Similarly, the second combination also uses ShieldIt Super, and implemented on polydimethylsiloxane (PDMS) substrate. The LCPs are designed based on two categories of unit cells namely: (a) solid type (two types) and (b) loop type (two types). The polarizers are evaluated via simulations and measurements in terms of i) conversion efficiency defined by its 90% conversion efficiency limits and its and fractional bandwidth $(BW)_{CE}$ and ii) axial ratio (AR) and associated fractional bandwidth, $(BW)_{3\,dB}$ with at least 3 dB as a limit. The four designed polarizers are categorized in terms of the number of conducting textile layers: (i) bi-layered design (three types) and (ii) single layered design (one type). The solid type unit cells are designed based on: i) a swastika-shaped unit cell sized at 51.7 × 59.8 × 3.34 mm$^3$ ( $0.49\lambda_g \times 0.57\lambda_g \times 0.03\lambda_g$ ); and ii) an unloaded unit cell sized at and 46×56.17×3.34 mm$^3$ ( $0.60\lambda_g \times 0.73\lambda_g \times 0.04\lambda_g$ ). On the other hand, the loop type are designed based on: iii) a crossed dodecagonal unit cell sized at 54 × 64 × 3.34 mm$^3$ ($0.51\lambda_g \times 0.61\lambda_g \times 0.03\lambda_g$ ), and iv) a square loop unit cell sized at 48 × 46 × 3.34 mm$^3$ ($0.45\lambda_g \times 0.43\lambda_g \times 0.03\lambda_g$ ), respectively. The dodecagonal design showed the highest $(BW)_{CE}$ which is 48.12 % (from 1.578 GHz to 2.578 GHz), compared to 23.88 % (2.36 GHz to 3 GHz) and 47.34% (1.58 GHz to 2.56 GHz) shown by the unloaded and the square loop design, respectively. Meanwhile, the highest measured axial ratio bandwidth $(BW)_{3\,dB}$, is 33.57% (from 1.71 GHz to 2.4 GHz) exhibited by the square loop-shaped design, followed by the unloaded unit cell design with 32.64%, dodecagonal design with 29.09% and the swastika design with 1.64%. To quantify their performance when integrated with the deployment mechanism, the performance of the polarizers are additionally assessed under different bending configurations and oblique incidences. In general the loop type designs have shown higher performance than the solid type designs.

# CHAPTER 1 INTRODUCTION

## 1.1 Introduction

These days satellites are widely used in our day to day life. Due to advancement in picosatellites, a contemporary class of picosatellites have been developed which is called as Cube Satellites, or CubeSat. They are classically placed into the low earth orbit (LEO) extending from 160 km to 2000 km height from the Earth (Babuscia et al., 2013; Shirvante, Johnson, Cason, Patankar, & Fitz-Coy, 2012). CubeSats are miniature in size, with single unit sized at 10 cm ×10 cm ×10 cm (referred as 1U), and a mass of nearly a kilogram, consumes less power, robust, inexpensive and fast. It is normally designed with single or multiples of 1U. Special attention must be provided in fulfilling the specification of the launcher when CubeSat is in its deployed condition (Lokman et al., 2017). An example is that in the Tropical Rainfall Measurement Mission (TRMM), the incomplete measurements due to less number of deployed measured components is solved using CubeSats (Peral et al., 2015)

Due to different attractive attributes, CubeSat is being deployed for numerous applications such as : a) earth and climate observation (2-4 GHz), b) space weather forecasting (2-4 GHz), c) space research, (0.4-0.45 GHz) and d) communications (18-27 GHz (Chahat, Hodges, Sauder, & Thomson, 2016; Chahat, Hodges, Sauder, Thomson, & Rahmat-Samii, 2016; Chahat, Sauder, Hodges, & Thomson, 2017; Costantine et al., 2015; Gordon et al., 2017; Hodges, Chahat, Hoppe, & Vacchione, 2017; Lokman et al., 2017; Shirvante et al., 2012). In 2013, Federal Communications Commission (FCC) released a notice for frequency allocation for S-band to be used in CubeSat application, it is from 2.39 GHz to 2.45 GHz (Federal Communications Commission, 2013). In

general, CubeSats used circular polarization (CP) for downlink and uplink frequencies. One of the main challenges, that require careful design is CP antenna as it is complex in design and gain is also very less(Ieee & Ieee, 2018; Lee et al., 2018).

Antennas in CubeSats communication systems is not only used for receiving but also for transmitting, especially when an adaptive power control is present. An under-performing antenna may increase power consumption and hence shorten the already limited battery life or solar power remarkably on CubeSats. Unnecessary losses might still occur when the polarizations of the linearly-polarized transmitting and receiving antennas are not matched(Heidt, Puig-Suari, Moore, Nakasuka, & Twiggs, 2000; Jones, Member, Grey, & Daneshmand, 2018; Lee et al., 2013). It follows the reciprocity theorem that a transmitter antenna behaves the same as an identical receiving antenna and vice versa. Fortunately, power losses due to polarization mismatch can be avoided by employing circularly polarized (CP) antennas. The polarization type is independent on the mutual orientation of the transmitting and receiving antennas and is relatively easy to implement in wearable applications as the size of the antenna is not as strictly limited than in handheld devices. There are mainly two cases when CP antennas are, if not essential, at least necessary to consider in wearable communication systems. The first is in satellite systems that are used for navigation and communication. Since satellite antennas often transmit CP waves, by employing CP receiving antenna, 3 dB better power level can be achieved compared with linearly polarized antennas("Advanced Antennas for Small Satellites," 2018; Freeman, 2019; Pan et al., 2015; Veljovic & Skrivervik, 2019).

The second case where CP antennas are beneficial includes communication with low power levels and orbiting CubeSats. This results in a varying orientation of the transmitting and receiving antennas. If polarizations of both transmitting and receiving

antennas are close to linear, the connection might be totally lost when a CubeSats moves in such a position where one antenna's orientation is perpendicular with respect to the other from a polarization perspective. Circular polarization is sensitive to distortion due to undesired reflections and hence, a system employing CP antennas is at its best in a line of sight connection. This usually is the case in satellite communication systems. In some cases of Global Positioning System (GPS) application(Rycroft, 1997), these antennas may also operate in multipath environment with linearly polarized antennas. On the other hand, a CP receiving antenna is blind to reflected, interfering signals because the handedness of the CP is often changed in reflection. Another disadvantage is that designing a CP antenna may be more challenging compared with a design process in which the polarization preference requirement is ignored. Depending on the structure and the chosen antenna topology, generating a CP wave may require special feeding techniques(Mohammad, Islam, & Member, 2018; Veljovic & Skrivervik, 2019).

Hence, instead of designing CP antennas, a linearly polarized antenna can be designed to be used in combination with a linear-to-circular polarizer to convert linearly polarized (LP) to CP. The use of linear-to-circular polarizer can solve the stringent CP antenna design problems, as well as enhance the gain of the LP antenna used in CubeSats. This will reduce the need of additional amplifier on board. Moreover, flexible design will enable deployment process of the polarizers

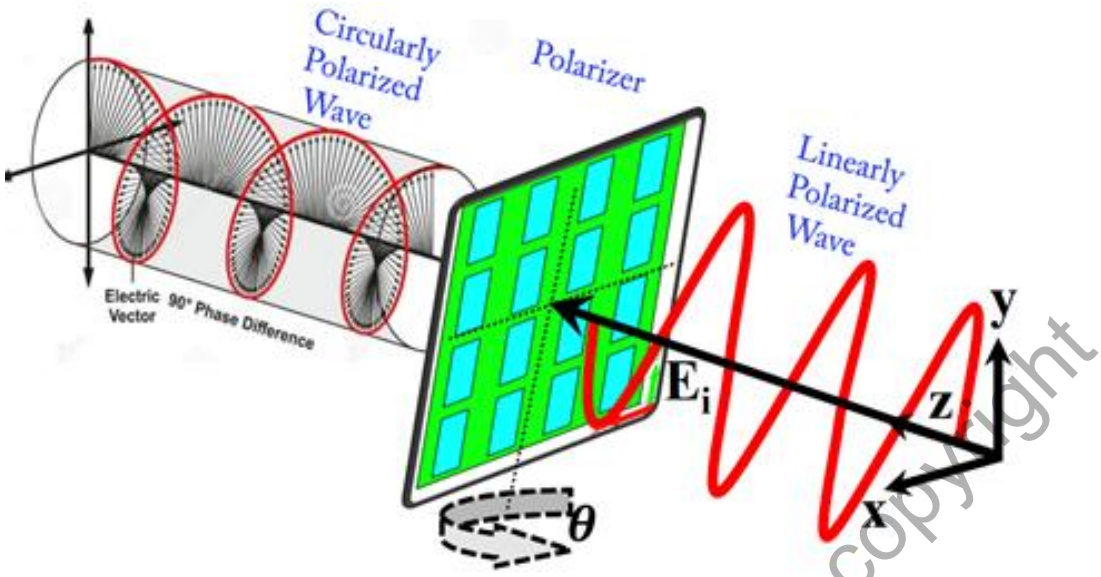


Figure 1.1 Conceptualized figure of linear to circular polarizer.

## 1.2 Problem Statement

Traditionally, a single feed, circularly-polarized (CP) antenna can designed using a patch antenna with a pair of corner truncation(Sharma, Gupta, & Chaudhary, 2015) . Moreover, other techniques also require the introduction of more than one port to enable circular polarization. More advanced techniques in realizing such antennas include the use of PIN diodes to reconfigure between linear and circular polarization. However, such methods need external biasing components and additional hardware. Most importantly, introducing high gain and broadband CP antennas in size-constraints of CubeSats is challenging (Lokman et al., 2017). The use of linear-to-circular polarizer mounted on the LP transmitting antenna can be considered as a functional alternative to achieve CP characteristics and avoid more complex CP antenna designs. When implemented on flexible materials, such polarizers can be used in CubeSats as the polarizer can be stowed in a compact form during launch, before being deployed for use in space. These CubeSats are increasingly deployed in large numbers for specialized purposes such as localization

and tracking, space research, earth observation, Science, Technology, Engineering and Mathematics (STEM) education (Babuscia et al., 2013; Lokman et al., 2017; Sakovsky, Pellegrino, & Costantine, 2017; Shirvante et al., 2012). Most recently, polarizers are designed based on unit cells in the form of loops, meander lines, dipoles (Sohail, Ranga, Esselle, & Hay, 2013), besides using metamaterial-based resonators (H.-X. Xu, Wang, Qi, Cai, & Cui, 2013b; H. X. Xu et al., 2016; H. X. Xu, Wang, Liang, Qi, & Gao, 2013). However, these polarizers are designed on conventional rigid substrates and surfaces. Different deployment process of CubeSat antennas are demonstrated in different literatures including tape-spring model deployment in (Heidt et al., 2000), umbrella like structure in inflatable mechanism in (Freeland, 1997). Among these deployment processes, flexible polarizers can be deployed using mechanical deployment as it is followed in (Freeman, 2019; Hodges, Hoppe, Radway, & Chahat, 2015) . There is a need for flexible polarizers due to their potential application in deployable CubeSats antennas, where the polarizer can be folded and stowed, before being deployed and launched. However, no flexible polarizers have been reported to the best of author's knowledge. In such applications, the performance change in deployed condition of the polarizer is need to be assessed to ensure their functionality upon deployment, in the cases of bent and oblique scenario.

Besides that, a large number of polarizers are also implemented in more than a layer with large gaps to obtain the best linear-to-circular conversion such as (Dietlein, Luukanen, Popović, & Grossman, 2007; Martinez-lopez, Rodriguez-cuevas, Martinez-lopez, & Martynyuk, 2014; Young, Robinson, & Hacking, 1973; W. Zhang, Li, & Wang, 2016) with four layers and dual layers (Fartookzadeh & Armaki, 2016). To get the suitable linear-to-circular polarization, these multi-layered structure inherits the complexity of maintaining proper gap between layers. The deviation of the gaps creates

conversion degradation of the polarizer. Moreover, polarizers implemented in a double sided topology also adds to fabrication complexity, as unit cells on both sides of the substrate need to be aligned with care to ensure proper operation. In the case of polarizer based structures, four types are discussed in (Munk, 2000) namely: (a) N-poles, (b) loop types, (c) solid interior or plate type and, (d) combination of these three types. It was argued that the loop type structures provided better performance among them. This thesis attempts to validate the performance of loop type linear-to-circular polarizer by comparing it to the solid interior type linear-to-circular polarizer on the basis of their axial ratio, conversion efficiency and phase difference between two orthogonal components of the transmitted wave.

These low-profile linear-to-circular polarizers are designed using different flexible materials, which is expected to be able to be stowed and deployed for use in a S-band CubeSat.

## 1.3 Thesis Objectives

This main aim of this thesis is to design solid interior and loop type unit cells on flexible linear-to-circular polarizer for space-constrained devices and applications. This is followed by the performance comparison of these two types of structures in such applications. Specifically, the objectives of the project are listed as follows:

- To design flexible linear-to-circular polarizers for S-band CubeSat application using solid-type and loop-type unit cells.
- To investigate the designed polarizers and evaluate them in terms of conversion efficiency and axial ratio in both normal and oblique incidences.

- To design and investigate compact, single layered polarizers under bending scenario and propose a suitable deployable mechanism for them.

## 1.4 Scope of Work

The design of the linear-to-circular polarizer starts with the design of a single unit cell design on flexible substrates and conductive material. Performance wise, the highest possible 3dB fractional axial ratio bandwidth (3dBFBW), $BW_{3dB}$ and conversion efficiency are considered to enable a circular polarization feature for the unit cell design. Two types of structures are designed in this thesis, namely a) solid interior type and b) loop type. Four different structures are presented in this thesis. The first two designs are based on solid interior type, while the last two designs are based on loop type design. The first two types are our preliminary designs for the initial research while the results of the last two types are more favourable for CubeSat application as they have achieved a higher axial ratio and conversion efficiency bandwidth. The first solid type design is a swastika-shaped structure, whereas the second one is based on two diverse loading phenomena namely a) loaded and b) unloaded circular structures. The third design is a dodecagonal-shaped structure with a combination of crossed structure in its centre. Finally, a square-loop-shaped design has been used for as the fourth design.

Next, each unit cell is optimized before being duplicated into a (4×4) array form. The functionality of the proposed polarizers are assessed via axial ratio and conversion efficiency from 2.39 GHz to 2.45 GHz for application in S-band CubeSat. Each type of polarizer is also designed, optimized and evaluated on two different flexible materials, on felt and polydimethylsiloxane (PDMS) substrates, and using a common conductive textile, ShieldIt Super. Considering the flexible nature of the linear-to-circular polarizers, additional evaluations of their performance when illuminated under oblique incidences

(from -45° to + 45°) as was performed in (Doumanis, Goussetis, Gómez-Tornero, Cahill, & Fusco, 2012; Fei, Shen, Wen, & Nian, 2015) and bending evaluations (with a 70 mm hypothetical cylinder according to) (Giman et al., 2017a; Hussin et al., 2017; Lago et al., 2017; Ramli et al., 2017a) are conducted to ensure their functional tolerance in practical implementations.

## 1.5 Contributions

This main contribution of this thesis is listed as follows:

Four innovative designs of flexible linear-to-circular polarizers for CubeSat application are presented based on solid- and loop-type designs, fabricated using felt textile and PDMS substrates.

All designs are broadband and operated within the S-band for CubeSat applications, with acceptable performance in terms of fractional bandwidth (with at least 90 % conversion efficiency) and 3 dB axial ratio in flat condition. A brief detail of the performance of different designs in flat condition are as follows:

i. The first solid interior type swastika-based structure produced a fractional bandwidth $(BW)_{CE}$ of 7.35 % and 5.29 % (from 2.39 GHz to 2.52 GHz) of 3 dB axial ratio bandwidth, $BW_{3dB}$.
ii. The second design (solid interior type) of unloaded structure produced a fractional bandwidth $(BW)_{CE}$ of 23.88 % and 39% (from 1.94 GHz to 2.88 GHz) of 3 dB axial ratio bandwidth, $BW_{3dB}$.
iii. The third design (loop type) is of crossed dodecagonal structure which has produced a fractional bandwidth $(BW)_{CE}$ and 3 dB axial ratio bandwidth, $BW_{3dB}$ of 48.12 % from 1.578 GHz to

2.578 GHz), and 35.23 % (from 1.66 GHz to 2.37 GHz), respectively.

iv. For the fourth design (loop type), the fractional bandwidth $(BW)_{CE}$ is 47.34 %, while the 3-dB axial ratio bandwidth, $BW_{3dB}$ is 33.94% (from 1.76 GHz to 2.48 GHz).

Besides that, the equivalent circuit model of each design is proposed and their performance validated with full wave electromagnetic (EM) simulations, followed by a discussion on the current distribution at the centre frequency of the respective operational bandwidth is presented. Besides that, comprehensive assessments of the proposed polarizers under bent and oblique conditions based on their expected practical implementation in post-deployment process is presented. Finally, a set of suggested precautionary steps of deployment is also explained.

## 1.6 Thesis Outline

This thesis is structured into five chapters. Chapter 1 introduces the thesis background, problem statement as well as objectives and thesis outline.

Chapter 2 reviews the theory of basic polarizers, before presenting a literature survey of the recent polarizers available in literature. An initial comparison of the designed polarizers in this thesis is also presented.

Chapter 3 explains the methodology of designing two different types of polarizers (solid type and loop type), the type of materials used, the fabrication procedure, and finally the measurements performed using specialized equipment and anechoic chamber.

Chapter 4 presents the simulation and measurement results of solid type and loop type polarizers, including the discussion of their performance. Besides that, their operation

under bent conditions and oblique incidences are also evaluated. The equivalent circuit model's results are also presented.

Finally, Chapter 5 concludes the thesis and presents several suggestions for future improvements.

# CHAPTER 2

# LITERATURE REVIEW

## 2.1 Introduction

This chapter discusses the literatures related to linear-to-circular polarizers. Section 2.2 describes different types of polarizations, followed by some basic parameters to assess linear-to-circular polarizer in Section 2.3 to Section 2.5. Different types of structures are then presented with a focus on single layered and multilayered design in Section 2.6 followed by a summary in Section 2.7.

## 2.2 Types of Polarization

Polarization is simply defined by the polarization ellipse, the form of the contour drawn from the tip of the electric field vector, as shown in Figure 2.1. Axial ratio states the character of the polarization ellipse and tilt angle states its orientation.

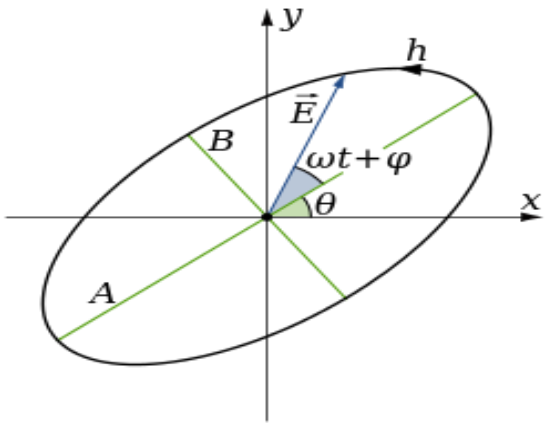


Figure 2.1 Ellipse Polarization (Balanis, 2005).

Meanwhile, the direction of the electric field vector is the sense of polarization in the path of propagation (Balanis, 2005). Polarization can be classified into three types; linear polarization, circular polarization or elliptical polarization. Polarization essentially depends on the features of the polarization ellipse. If the minor axis is equal to major axis of the ellipse, a circular polarization will be obtained. However, if there are difference between both axes, with zero minor axis, the wave changes into a straight line and is defined as linearly polarized waves (Balanis, 2005). Figure 2.2 illustrates the three different types of polarization.

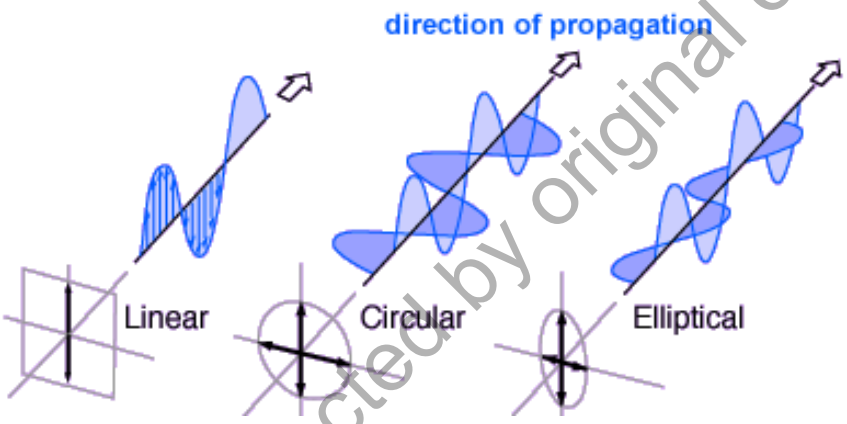


Figure 2.2 Different types of polarization (Balanis, 2005).

On the other hand, polarization of an antenna is defined as the polarization of the electromagnetic (EM) waves that radiate in the far field of the antenna. The EM wave is basically the combination of both electric and magnetic fields (Balanis, 2005). Each polarization has their own characteristics. For a linearly polarized antenna, it is defined by the tilt angle of the polarization ellipse, denoted by $\tau$. Linear polarization are classified by in terms of its sense: (i) 90º or vertical, (ii) 0º or horizontal, and (iii) ± 45º or slant. Meanwhile, for a circularly polarized antenna, the sense is specified by the nature of the movement of the electric field vector tip, either in clockwise (RHCP) or counter-clockwise (LHCP) directions, as shown in Figure 2.3.

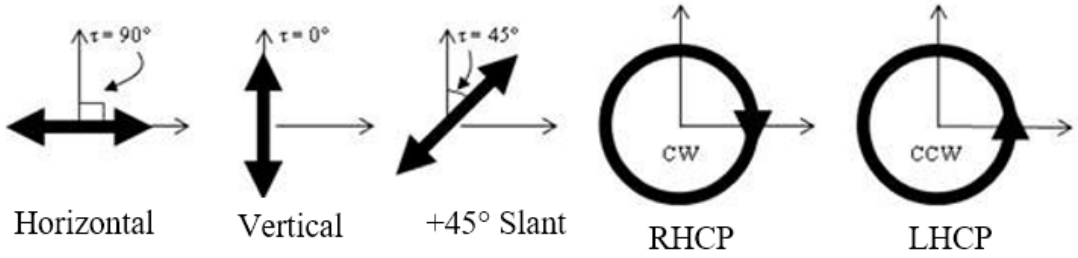


Figure 2.3 Different time-varying directions of electric field for different polarizations (Balanis, 2005) .

In linear-to-circular polarizers, an incident linearly polarized wave (LPW) is considered, whose E field vector $E_i$ is pointed towards an angle $\varphi$ = 45° of $x-$ axis, and travels through the $z-$ axis as shown in Figure 2.4 (Martinez-lopez et al., 2014).

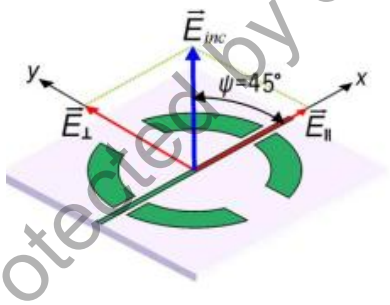


Figure 2.4 Orientation of incident electric field (Martinez-lopez et al., 2014).

The field component is decomposed into two orthogonal components $E_x$and $E_y$ .(Di Palma et al., 2017; Fartookzadeh & Armaki, 2016; Martinez-lopez et al., 2014; J. Zhang, Yin, & Ma, 2009a; H. L. Zhu, Cheung, Chung, & Yuk, 2013). The ratio between two orthogonal components can be given as; $q = \frac{|E_x^i|}{|E_y^i|}$ Instead of $E_x$ and $E_y$, $T_x$ and $T_y$ is used to indicate the transmission signals The translation of $E_x$ and $E_y$ to $T_x$ and $T_y$ is facilitated using Equation (2.1) (Di Palma et al., 2017; Fartookzadeh & Armaki, 2016; Khan & Eibert, 2019):

$$\left|E_x^i\right|.|T_x| = q\left|E_y^i\right|.\left|T_y\right| \quad (2.1)$$

The value of $q$ ranges from 0 to 1, for purely circularly polarized wave the $q = 1$ and the phase is given by;

$$\left[\Phi\left(E_x^i\right) + \Phi(T_x)\right] - \left[\Phi\left(E_y^i\right) + \Phi\left(T_y\right)\right] = \pm n\frac{\pi}{2} \quad (2.2)$$

where $\Phi$ represents the phase of the respective parameter in the subscript of $n = 1,2,3$. If it is assumed that $E_x^i$ and $E_y^i$ have equal phase and magnitude, then circular polarization can be written as;

$$|T_x| = \left|T_y\right| \quad (2.3)$$

$$\Phi\ (T_x) - \ \Phi\ \left(T_y\right) = 90^0 \quad (2.4)$$

When the conditions from equations (2.3) and (2.4) are met, the linearly-polarized wave's incident to the polarizer will transform to circularly polarized waves while transmitting from the other side of the polarizer. It is obvious from equations (2.3) and (2.4) that the polarizer can be characterized by the evaluation of transmission coefficient in terms of magnitude and phase.

All polarizations has an orthogonal counterpart; vertical and horizontal, RHCP and LHCP, ± 45º angle. Moreover, each polarization can be designed out of any two orthogonal polarizations(Stutzman & Thiele, 2012) .

## 2.3 Axial Ratio

The CP characteristics of transmitted wave from a linear-to-circular polarizer is characterized by axial ratio which defines the ratio between two orthogonal components of the transmitted wave. These two components are termed as horizontal and vertical components. The criteria of CP are fulfilled when the ratio between the magnitude of

these two components has a vale near to unity. In terms of logarithmic scale, a 3dB threshold is allowed to design broadband linear-to-circular polarizer. The axial ratio can be calculated using equation 2.5 (Baena, Glybovski, Del Risco, Slobozhanyuk, & Belov, 2017; W. Zhang, Li, & Xie, 2017), where $T_x$ and $T_y$ are transmission coefficients for x and y polarized waves respectively.

$$AR = \sqrt{\frac{|T_y|^2 + |T_x|^2 + |T_y^2 + T_x^2|}{|T_y|^2 + |T_x|^2 - |T_y^2 + T_x^2|}} \tag{2.5}$$

The AR indicates the CP characteristics of the transmitted wave from the linear-to-circular polarizer. Theoretically, 0 dB is the ideal value to represent the CP characteristics however, 3 dB is assumed to be the threshold for wideband designs to fulfil CP characteristics.

## 2.4 Conversion Efficiency

To assess the ability of a linear-to-circular polarizer to convert linear waves to circular waves, conversion efficiency and conversion coefficient are two important parameters used by researchers in (Sohail et al., 2013; Wang, Shen, Wu, & Feng, 2015; Yan & Vandenbosch, 2013). If the circular conversion coefficient for right-handed circular polarization (RHCP) wave, $C_-$, and left-handed circular polarization (LHCP) wave, $C_+$, are expressed using equations (2.5) and (2.6), then the conversion efficiency $\eta_{conv}$ can be given by equation (2.7) (Mirza, Hossain, et al., 2018; Mutlu, Akosman, Kurt, Gokkavas, & Ozbay, 2012; Sohail et al., 2013; Wang et al., 2015; H.-X. Xu, Wang, Qi, Cai, & Cui, 2013a; Yan & Vandenbosch, 2013; W. Zhang et al., 2016);

$$C_+ = E_x^i T_x - jE_y^i T_y \tag{2.6}$$

$$C_- = E_x^i T_x + jE_y^i T_y \tag{2.7}$$

$$\eta_{conv} = \frac{(|C_-|^2 - |C_+|^2)}{(|C_-|^2 + |C_+|^2)} \times 100 \quad (2.8)$$

Parameters $|C_-|$ and $|C_+|$ are the magnitude of circular conversion coefficient for right-handed circular polarization (RHCP) wave, $C_-$ , and left-handed circular polarization. Conversion efficiency is a measure of how efficiently the polarizer is converting the LP to CP. Ideally, a high conversion efficiency over broad frequency range at normal incident angle is preferred.

## 2.5 Ellipticity

Ellipticity (presented in Equation 2.9) defines whether the wave is linearly polarized or purely circularly polarized. The value of $\eta$=0˚ indicates a pure linearly polarization, whereas $\eta$=45˚ shows a purely circularly polarization (Balanis, 2005; Mirza, Hossain, et al., 2018; Mutlu et al., 2012; Sohail et al., 2013; Wang et al., 2015; H.-X. Xu et al., 2013b; Yan & Vandenbosch, 2013; W. Zhang et al., 2016). $C_+$ and $C_-$ is representing RHCP and LHCP wave.

$$\eta = tan^{-1}\left(\frac{abs(C_+) - abs(C_-)}{abs(C_+) + abs(C_-)}\right) \quad (2.9)$$

### 2.5.1 Theory of Linear-to-circular polarizer

The conceptualized depiction of the linear-to-circular polarizer has been presented in Figure 2.5. The incident electric field is depicted as $E_i$ and transmitted electric field is shown as $E_t$.

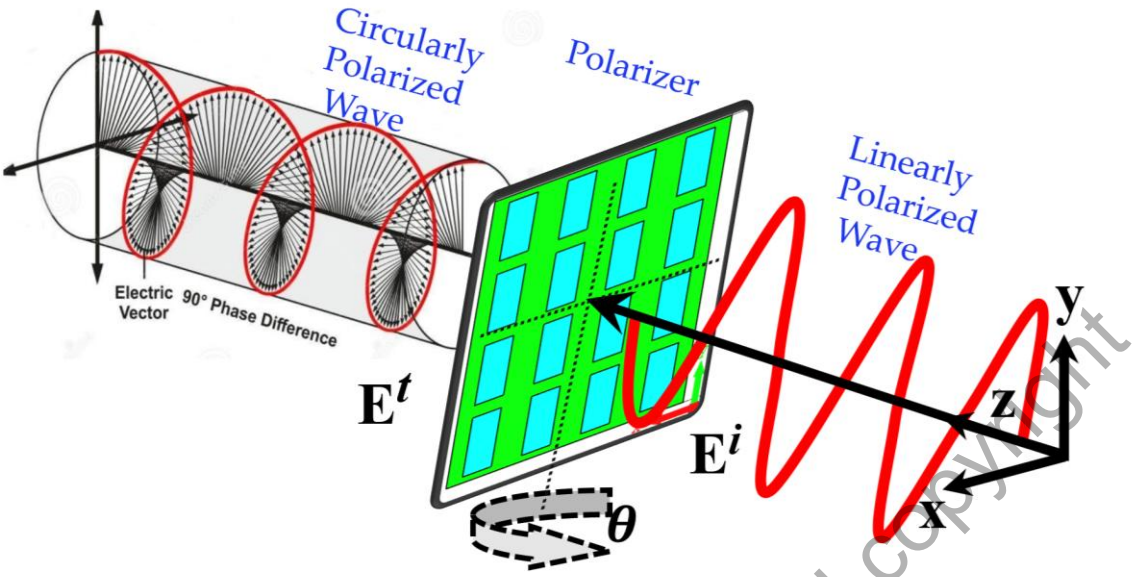


Figure 2.5 Conceptualized working of linear to circular polarizer.

A linearly-polarized-wave (LPW) impinging on the linear-to-circular polarizer in the direction of +$z$-axis whose electric field $E^i$ is polarized at $\Phi$=45˚ is first considered. This wave can be decomposed further into two orthogonal components, $E_x^i$ and $E_y^i$, representing the components of $E^i$ towards the $x$- and $y$-axis, respectively. Meanwhile, $E_x^t$ and $E_y^t$ are for the transmitted electric field, $E^t$ when $\Phi$=45˚ it produces maximum circular polarizer.

## 2.6 Different Types of Unit Cells

Periodic structures, or arrangements of equally spaced, identical elements, have been of interest in many areas of physics and engineering. Although being rather established from a mathematical point of view, periodic structures are being rapidly developed in recent years for practical applications. This is because they can be optimized in terms of unit element design and their placement in a periodic array to exhibit certain characteristics to suit particular requirements .

The unit cells are built to "tailor" electromagnetic waves in the free-space environment. Acting as a barrier for the waves propagating along the link, the unit cells controls the flow of the electromagnetic energy. The transfer function of the unit cell manipulates the EM wave. As a result, some of the frequency constituents of the wave are blocked, and some pass through the unit cell fence. The unit cells can be categorized into four major types, based on the shape of the elements used, as illustrated in Figure 2.6 , as follows:

1) The centre connected or N-poles, such as dipole, three-legged element.

2) Loop type such as the three- and four-legged loaded elements, circular, square and hexagonal loops.

3) Plate type with solid interior.

4) The combination of them.

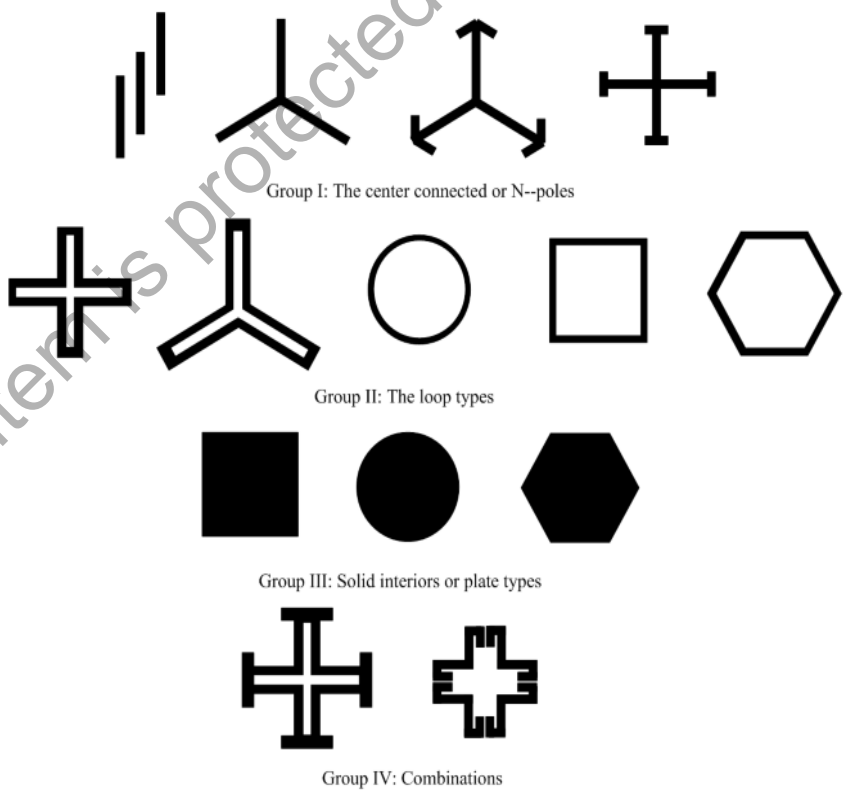


Figure 2.6 Typical polarizer elements classified in four major groups (Munk, 2000).

The most preferred type unit cell by is the loop family. Unit cell designs with loaded and unloaded elements have been used. If the gap in the metallic sheet is small, then value of the capacitance is high. On the contrary, if the slot is large, then the capacitance is small and this is termed as a capacitive loaded element, as shown in Figure 2.7. These are

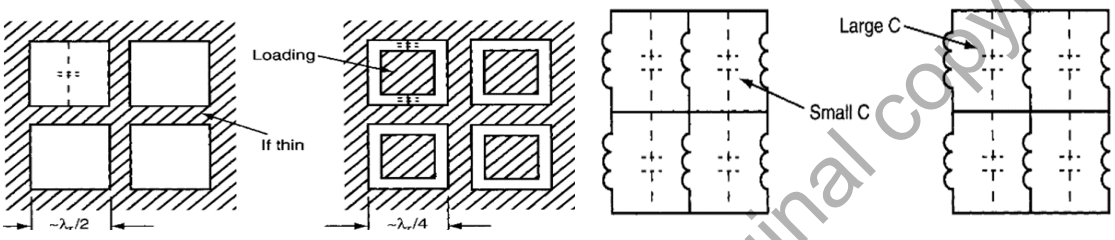


Figure 2.7 Loaded and unloaded unit cells with gap capacitance (A. Munk, 2000).

A summary of CP antenna with metasurface has been presented in Table 2.1. (Z. Wu, Li, Li, & Chen, 2016) has achieved a $BW_{3dB}$, 3 dB axial ratio fractional bandwidth, $BW_{3dB}$ of 16.5 % with a size of $0.56\lambda_0 \times 0.45\lambda_0 \times 0.06\lambda_0$ as compared to 8.0% in (H. Zhu, Chung, Sun, Cheung, & Yuk, 2012) with a size of $0.96\lambda_0 \times 0.96\lambda_0 \times 0.0745\lambda_0$. The first design has used square shaped CPW in the front plane while the second design has used unloaded square loop with diagonal metal strips. A higher fractional bandwidth has been achieved by (Cao, Cheung, Yuk, & Zhu, 2015) using Jerusalem-cross-based defected ground structure. In this case the fractional bandwidth fulfilling has a value 27.5% (1.41 GHz to 1.86 GHz) with a size of $0.44\lambda_0 \times 0.39\lambda_0 \times 0.07\lambda_0$. The highest CP antenna with metasurface has been presented by 40.2% in (Agarwal, Nasimuddin, & Alphones, 2012) with a size of $0.72\lambda_0 \times 0.6\lambda_0 \times 0.28\lambda_0$.

Table 2.1 Summary of the CP antenna with metasurface

| Ref | Design | Fractional bandwidth of Axial Ratio $BW_{3dB}$ | Frequency Range (GHz) | Technique Used | Size in $\lambda_0$ |
|---|---|---|---|---|---|
| (Z. Wu et al., 2016) | 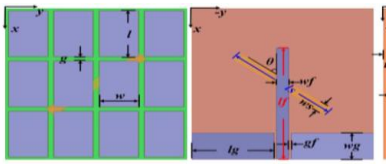 CPW feed, metasurface on top | 16.5% | 4.9-5.9 | Polarizer unit cell | 0.56×0.45×0.06 |
| (Z. Wu et al., 2016) | 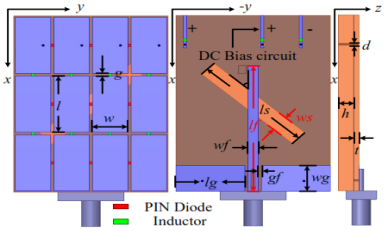  CPW feed, metasurface on top | 16.9% | 5.4 to 6.4 | Polarizer unit cell | 0.73×0.54×0.07 |
| Ref | Design | Fractional bandwidth of Axial Ratio $BW_{3dB}$ | Frequency Range (GHz) | Technique Used | Size in $\lambda_0$ |
| (Cao et al., 2015) | 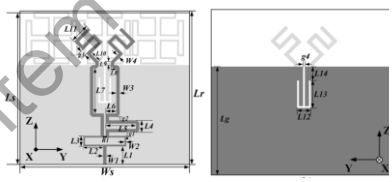 Left=top view right=bottom view<br>Using Defected ground structure using Jerusalem Cross unit cell | 27.5% | 1.41 to 1.86 | MS | 0.44×0.39×0.07 |

| | | | | | |
|---|---|---|---|---|---|
| (P. C. Wu et al., 2015) | 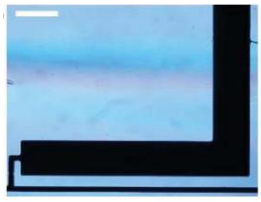 | NOT GIVEN | 7.5 to 25 | Not Given | NOT GIVEN |
| (Ta & Park, 2015) | 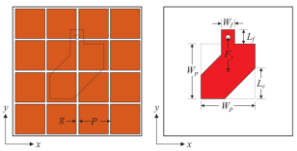 | 23.4% | 4.9-6.2 | MS | 0.58×0.58×0.056 |
| (Lin, Wong, Zhang, & Lai, 2014) | 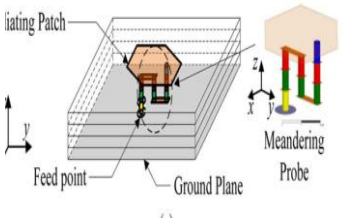 | 16.8% | 5.05-5.98 | Not Given | 0.66×0.66×0.14 |
| (Yang, Zhou, Yu, & Li, 2014) | 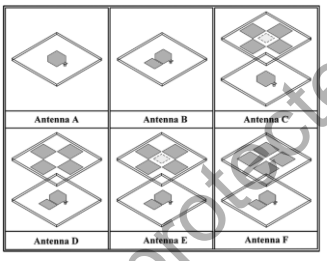 | 20.7% | 5.49-6.73 | Parasitic patches | 0.8×0.8×0.09 |
| (Bernard, Chertier, & Sauleau, 2011) | 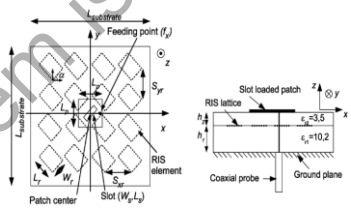 | 14.9% | 2.13-2.37 | Reactive Impedance Surface | 0.7×0.7×0.06 |
| (Nakamura & Fukusako, 2011) | 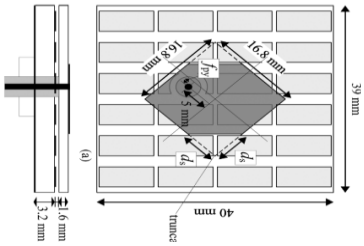 | 20.4% | 5.40–6.63 | Artificial Ground Structure | 0.27×0.28×0.01 |

| | | | | | |
|---|---|---|---|---|---|
| (H. L. Zhu et al., 2013) | 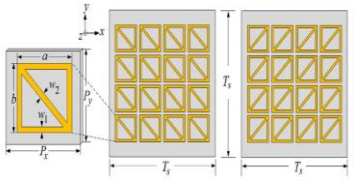 (L to R) unit cell,RH and LH | 8.0% | 2.4-2.6 | MS | 0.96×0.96 ×0.0745 |
| (Cai, Wang, Zhang, & Shi, 2015) | 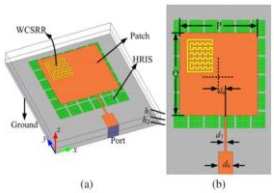 | 1.86% | 3.45-3.51 | MS | 0.46×0.51×0.028 |
| (Agarwal et al., 2012) | 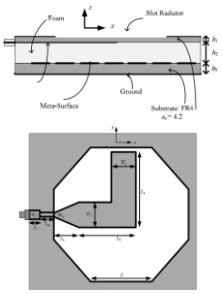 | 40.2% | 4.70-7.11 | MS | 0.72×0.6×0.28 |
| (Nasimuddin, Chen, & Qing, 2012) | 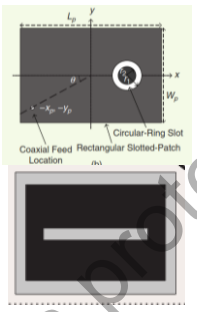 | 28.3% | 3.6-4.55 | MS | 0.82×1.18 ×0.06 |

### 2.6.1.1 Multi-Layered Linear-to-Circular Polarizers

The different linear-to-circular polarizers available in literature is presented in this section. The first example of unit cell is the split ring resonator to design linear-to-circular polarizer in (Martinez-lopez et al., 2014), as shown in Figure 2.8. The principle of operation of the linear-to-circular polarizer is described in detail, besides a proposed equivalent circuit model representation. The 3 dB axial ratio bandwidth, $BW_{3dB}$ of this

design is from 25.5 GHz to 36.5 GHz (35.48 %) with a size of 9.35 $\lambda_0$ × 9.35 $\lambda_0$ × 0.9 $\lambda_0$. This design uses four layers of array, which increases fabrication complexity.

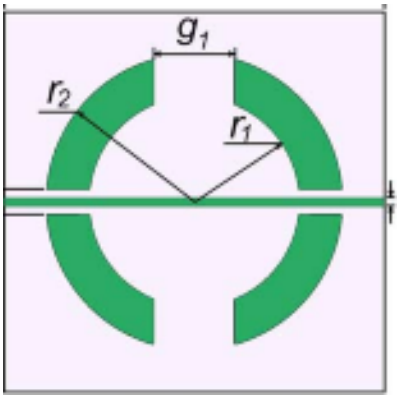


Figure 2.8 Split ring resonator bisected by a metal strip horizontally (Martinez-lopez et al., 2014)

Next, a classic meander-line shaped polarizer has been used to design a linear-to-circular polarizer, operating from 17 GHz to 23 GHz (Joyal, Riel, Demers, & Laurin, 2015). Different distances are used between the three layers, at $\lambda/4$ and $\lambda/8$. This design is optimized for oblique angles of incidence. This design produced a 3 dB AR fractional bandwidth, $BW_{3dB}$ of 30 %. This is achieved by cancelling the mode coupling of each layer. The drawback of this multi-layered structure is the large spacing between each layer, as illustrated in Figures 2.9.

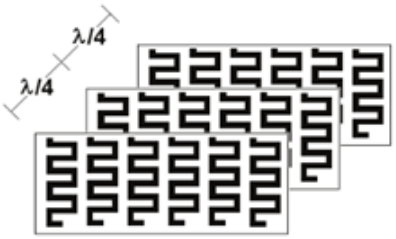


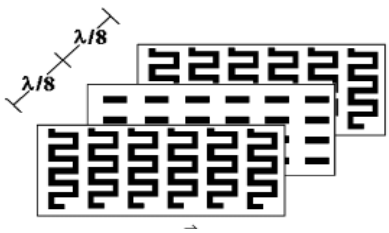

Figure 2.9 Meander-lined polarizer (a) meander-line with $\frac{\lambda}{4}$ and (b) meander-line with $\frac{\lambda}{8}$. (Joyal et al., 2015).

Besides that, an electromagnetic band gap (EBG) polarizer has been designed to convert the operation of a linearly polarized horn antenna into circularly polarized by mounting the polarizer in front of it in (Arnaud et al., 2010) , as shown in Figure 2.10. Besides the polarizing metallic grid, a metallic ground is also present in between the polarizer and the antenna. Due to this, there are two additional drawbacks of such design: a) there is a ground plane connect to the EBG antenna and b) the polarizer should be covered by spacers on both front and back sides.

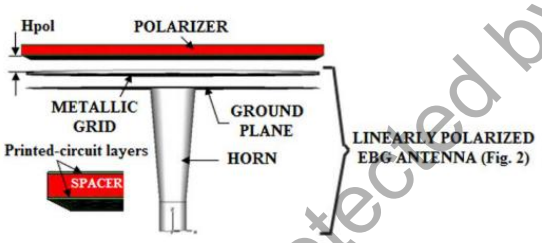


(a)

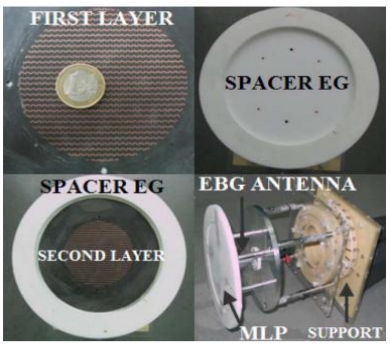


(b)

Figure 2.10 a) Simulation setup in CST (b) Antenna combined with polarizer. (Arnaud et al., 2010).

In (J. Zhang, Yin, & Ma, 2009b) (Figure 2.11), a multifunctional meander-line polarizer is presented. It is capable of converting linear to circular and linearly polarized horizontal waves to linearly polarized vertical waves. The polarizer uses four layers of meander-line slabs, and each slab is separated by a spacer which is 12 mm thick. The proposed polarizer is sized at 3.73 λ ×1.86 λ and is capable of linear-to-circular polarization conversion from 5.6 GHz to 10.4 GHz; with a $BW_{3dB}$ of 60 %.